PORT SAID ENGINEERING RESEARCH JOURNAL

Faculty of Engineering - Port Said University
Volume (28) No. 3 pp: 44:58

# Lateral Load Response of Reinforced Concrete Buildings Constructed on Clay Soil with Weak Zones

*Aya G. Abdel-Nasser [1, *], Emad Y. Abdel-Galil [2] and Ezzaat A. Sallam[3]*

[1]*Civil Engineering Department, Faculty of Engineering, Port Said University, Email: aya.gamal@eng.psu.edu.eg*
[2] *Civil Engineering Department, Faculty of Engineering, Port Said University, Email: emad0057@eng.psu.edu.eg*
[3] *Civil Engineering Department, Faculty of Engineering, Port Said University, Email: Ezzat.sallam@eng.psu.edu.eg*
**Corresponding author, DOI: 10.21608/PSERJ.2024.273104.1324*

*Received 4-3-2024*
*Revised 28-3-2024*
*Accepted 7-4-2024*



## ABSTRACT

Buildings in some conditions suffer from structural issues caused by foundation soil inhomogeneity. The main cause of an inhomogeneity in soil profile is the presence of voids or very weak large pockets. The present paper deals with the structural behavior of concrete buildings, exposed to transverse loading such as seismic loads, when constructed on clay soil with predefined weak zones (voids). The finite element program ANSYS was used to study the effect of an underground void of different sizes and locations. A comprehensive study of various parameters was conducted on six structures of different widths and heights, considering the underground void diameter and void location. The effects of underground voids on building natural periods and structural response to static lateral loads were investigated. According to the studied cases, it was found that the void effect in increasing the differential settlement almost fades at void eccentricity equals 1 to 3 times the structure width from the foundation center. Although the void effect in increasing lateral displacements at structure floor levels fades at void eccentricity equals 1 to 1.75 times structure width. The void effect approximately vanishes at void depth equals 1 to 3.5 times the structure width from the foundation level.

**Keywords**: Lateral loads, Underground void, Critical locations, building width, Finite element, Soil structure interaction.

## 1 INTRODUCTION

The construction projects in new urban areas such as south Port Said and East Port Said have been increased in last 5 years. The soil profiles in such areas may differ from downtown areas despite performing site investigations studies. These areas may have weak soil gaps or voids due to historical burying of organic materials. In other conditions, underground voids may be formed as a result of many reasons such as mining and tunneling works, ice lenses melting below the surface, the melting of soluble materials such as gypsum, salt, dolomite, and limestone, and the disintegration of methane hydrate [1]. Due to the prescribed problems, several research works in literature have investigated the effects of construction on soils containing voids below. The behavior of footings founded on soil containing underground voids under vertical static loads was investigated by many researchers [2-22]. These researchers studied several effective parameters such as the number of voids, void sizes, void locations, and foundation soil properties. Mansouri *et al.* [23] and Mazouz *et al.* [24] investigated the effects of the presence of voids near ground slopes under centric and eccentric loads. Many research works have studied how to reinforce the foundation soil beneath the footings to reduce the effects of underground voids [25-27].

There is a lot of research also examining the effect of the presence of underground voids or tunnels on the seismic response of the voids and the ground surface above. Sahoo and Kumar [28] investigated the stability of a long void formed in a cohesive frictional soil

subjected to pseudo-static horizontal earthquake body forces. Asakereh *et al.*[29] conducted an experimental study of a foundation founded on unreinforced and geogrid-reinforced sand with a circular void subjected to a combination of static and repeated loading. Chakraborty and Kumar [30] used the lower-bound finite element limit analysis to investigate the stability of a long unsupported circular tunnel with the inclusion of seismic body forces. Chakraborty and Sawant [31] studied the seismic bearing capacity for foundations located above undrained clay containing an unlined tunnel using finite element. Zhang *et al.* [32] investigated the seismic behavior of strip foundations resting above purely cohesive containing square continuous void using an AFELA program with the pseudo-static approach for a variety of material properties and geometric parameters. Design tables and charts were presented from the results for use by engineers. Sadegh *et al.* [33] also studied the seismic behavior of a strip footing rested over an unsupported rectangular void with various horizontal seismic accelerations, soil properties and geometric factors for the void using machine learning (ML) techniques. All the research works mentioned above focused on the behavior of footings placed on soil with voids without considering the soil-structure interaction.

Few researchers studied the effects of the underground structures-soil-surface structure interaction subjected to static or dynamic loads. For the cases under static loads, Jao and Wang [34] used the finite element method to investigate the interaction between strip foundations and concrete-lined circular tunnels located centered under the strip footings. Mroueh and Shahrour [35] studied numerically the interaction between tunneling and an adjacent building in soft soils using a full three-dimensional simulation considering that the structure already exists during tunneling. Mirhabibi and Soroush [36] investigated the influence of surface structures on ground surface settlement of twin tunneling using a finite element program. Boldini *et al.*[37] presented a parametric study using the finite element method to investigate the effects of tunneling on the surface reinforced concrete frame structures with various numbers of stories, eccentricity, and length of the frame. Abdel-Nasser *et al.* [38] presented a parametric study using finite element software to investigate the response of different RC structures rested on clay soil containing voids of different sizes and locations. Equations are proposed for estimating the critical void locations under RC structures considering soil structure interaction.

For dynamic studies, Pitilakis *et al.* [39] conducted a set of numerical analyses to study the dynamic response of circular tunnels, considering the effects of the adjacent surface ground oscillating buildings. Abate and Massimino [40] investigated numerically the dynamic tunnel–soil–surface building interaction subjected to seismic inputs using finite element parametric analysis. Wang *et al.* [41] examined experimentally the seismic response of underground structures-soil-surface structures interaction law by using a shaking table test under various input parameters including seismic waveform and its peak acceleration.

Previous studies mainly studied the footing behavior due to the presence of underground voids without consideration of the soil-structure interaction and the behavior of nonlinearity of the surface concrete structure. The seismic response of structures is usually estimated by assuming fixed support at the structure foundation. This method is acceptable when the structures are founded on solid rock. The soil-structure interaction should be mainly considered when estimating the seismic response of the structures founded on soft soils, especially with underground voids. There is a clear lack of studies investigating three-dimensional fully reinforced concrete structures placed on soil with voids, considering the influence of the different sizes of structures (areas and heights). This topic needs more research considering the soil-structure interaction. The current study investigated the behavior and stability of the reinforced concrete structures placed on clay soil with underground voids subjected to equivalent seismic load, by using the finite element method. A three-dimensional full-scale simulation of six structures was considered with different structure areas and heights considering the interaction between the surface structure and the foundation soil. A wide range of void diameters and locations from the footing were considered in this study.

## 2 MATERIALS AND METHODS

Three-dimensional reinforced concrete structures were analyzed using a finite element program ANSYS. This analysis focused on studying the behavior of surface structures placed on clay soil containing voids in different locations. The structures were subjected to an equivalent static seismic load according to ECP-201 [42]. Half part of the symmetric models was simulated in ANSYS to reduce the number of elements of the analyses by using the "symmetry region" option. Six structures with different sizes were considered for this study. Loads, material modeling, and structural modeling used in this numerical analysis are presented in the following sections.

### 2.1 Material Modeling

Clay foundation soil was modeled using the Mohr-Columb model in ANSYS, which is characterized as an isotropic, linearly elastic-perfectly plastic model. The nonlinear concrete material model was used for modeling beams, columns members, and foundations. The stress-strain curve of the model is an ascending second-order branch and a descending branch oblique straight line in

the compression part and a linear model for the tensile part [43]. The model of elastic-perfectly plastic with a small slope was applied for modeling the reinforcement in beams and columns.

### 2.2 Structural Modeling

#### 2.2.1 Soil and Weak Zones Model

Soild185 element in ANSYS was used to model the clay soil block. The vertical and horizontal boundaries of the clay foundation soil model were chosen sufficiently far away to avoid any effects on the results obtained. The boundaries of the foundation soil were five times the footing length 5*B* laterally from the foundation edge and ten times the footing length 10*B* vertically beneath the ground surface. The vertical boundaries were set to be free in the vertical direction and the bottom surface of the soil block has been fixed in all directions. The density of soil elements was increased in the area around the footing and the void locations. The weak zone is defined as soil with young's modulus less than 10% of the parent surrounding soil. In the current analysis, the weak zone soil stiffness was totally neglected and the elements filling the weak area were removed. Figure 1 shows the mesh elements and the boundaries for the half part of the symmetric model.

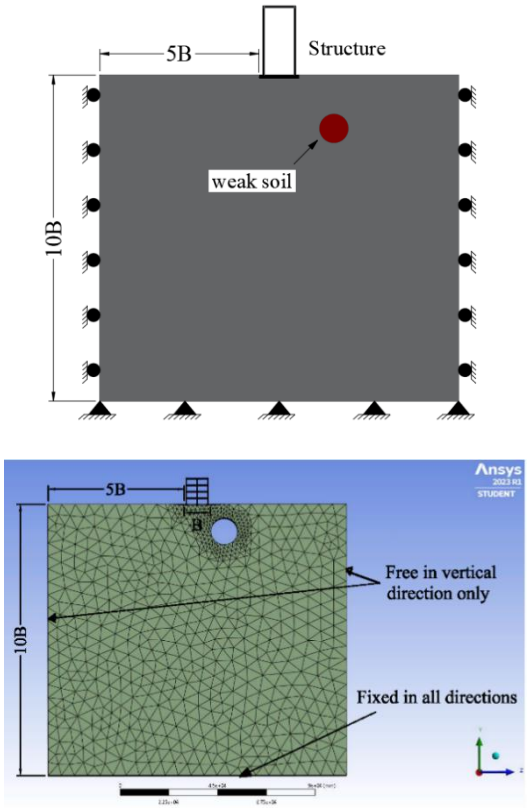


**Figure 1: Mesh elements of the half part of the symmetric ANSYS model and foundation soil boundaries**

#### 2.2.2 Reinforced Concrete Structure model

Solid 185 was chosen also to simulate the nonlinear concrete elements (foundations, columns, and beams elements). Reinforcement was modeled using the option of "reinforcement model type" in ANSYS as a beam element embedded in the concrete elements, as shown in Figure 2.

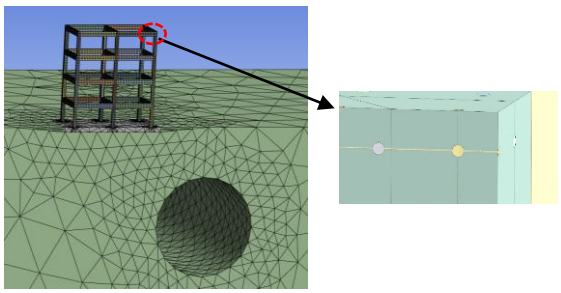

**Figure 2: Reinforced concrete structure model with "*reinforcement model type*" option.**

### 2.3 Verification of Numerical Model

For validation of the current ANSYS model, a case study from Badie [44] were selected and the experimental results were compared with those of the ANSYS model. An experimental model of strip footing with 51mm in width supported on soil with a centric void of 122 mm under the footing. The boundaries of the soil block were 366mm and 762 mm vertically and horizontally from the center of the footing, respectively, as the model test conducted by Badie [44]. The soil properties for the foundation soil in the test: Modulus of elasticity $E$= 19.86 MPa, Poisson ratio $\nu$ = 0.39, Soil cohesion $c$ = 158.7 kPa, Internal friction $\varphi$ = 8 degrees, Dry unit weight of the soil=13.5 kN/m$^3$. Figure 3 shows a comparison of the experimental load-settlement results performed by Badie [44], the finite element of the same model carried out by Badie [44] and Lavasan *et al.*[14], with the current model done by ANSYS. Good agreement was presented between the results of the present analysis with the literature's results.

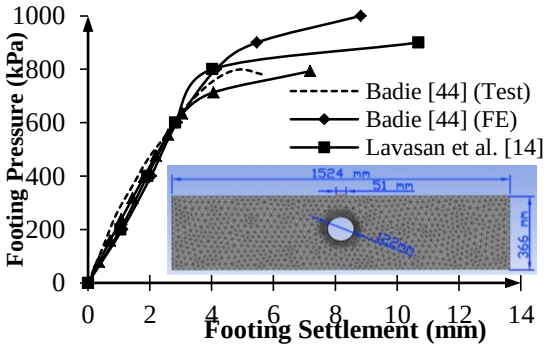


**Figure 3: Comparison of the load-settlement under the footing between the ANSYS model with models developed by Badie [44] and Lavasan *et al.* [14]**

### 2.4 Parametric Study

The aim of the parametric study is to investigate the effects of underground voids on the structural response of multi-story buildings. To perform this investigation and on the basis of the most critical mode of vibration of the value of lateral load is the fundamental mode, firstly, a modal analysis was performed followed by lateral load analysis.

#### 2.4.1 Building Descriptions

A wide range of parameters was considered in this study to study the effects of the presence of underground voids on the above-surface structures under seismic loads. The parameters included void diameter *D*, void depth *y*, void eccentricity from the footings *x*, and the raft's widths *B* and structure heights *H*.

A simulation of a 3D finite element model of reinforced concrete structures placed on clay soil containing a continuous circular underground void was performed using the ANSYS software. Figure 4 shows the six examined structures in the current analysis and Table 1 presents the values of the designed dimensions and the reinforcement of these structures.

**Table 1. Dimensions and reinforcement of all structures.**

| ST. | ST 1 | ST 2 | ST 3 |
|---|---|---|---|
| Slabs ($m^2$) | 10*10 | 20*20 | 30*30 |
| St. height *H* (m) | 12 | 12 | 12 |
| Number of floors | 4 | 4 | 4 |
| Raft Area ($m^2$) | 12.5x12.5 | 22.5x22.5 | 32.5x32.5 |
| Raft depth $t_s$ (m) | 0.6 | 0.6 | 0.6 |
| Beams ($m^2$) | 0.3x0.6 | 0.3x0.6 | 0.3x0.6 |
| External columns ($m^2$) with RFT | 0.4x0.4 8φ 18mm | 0.4x0.4 8φ 18mm | 0.4x0.4 8φ 18mm |
| Internal columns ($m^2$) with RFT | 0.4x0.4 8φ 18mm | 0.4x0.4 8φ 18mm | 0.4x0.4 8φ 18mm |
| Top beam RFT | 3φ 16mm | 3φ 16mm | 3φ 16mm |
| Bottom beam RFT | 3φ 16mm | 3φ 16mm | 3φ 16mm |

| ST. | ST 4 | ST 5 | ST 6 |
|---|---|---|---|
| Slabs ($m^2$) | 10*10 | 20*20 | 30*30 |
| St. height *H* (m) | 30 | 30 | 30 |
| Number of floors | 10 | 10 | 10 |
| Raft Area ($m^2$) | 12.5x12.5 | 22.5x22.5 | 32.5x32.5 |
| Raft depth $t_s$ (m) | 1 | 1 | 1 |
| Beams ($m^2$) | 0.3x0.6 | 0.3x0.6 | 0.3x0.6 |
| External columns ($m^2$) with RFT | 0.4x0.4 8φ 25mm | 0.4x0.4 8φ 25mm | 0.4x0.4 8φ 25mm |
| Internal columns ($m^2$) with RFT | 0.5x0.7 12φ25mm | 0.5x0.7 12φ25mm | 0.5x0.7 12φ25mm |
| Top beam RFT | 3φ 16mm | 3φ 16mm | 3φ 16mm |
| Bottom beam RFT | 3φ 16mm | 3φ 16mm | 3φ 16mm |

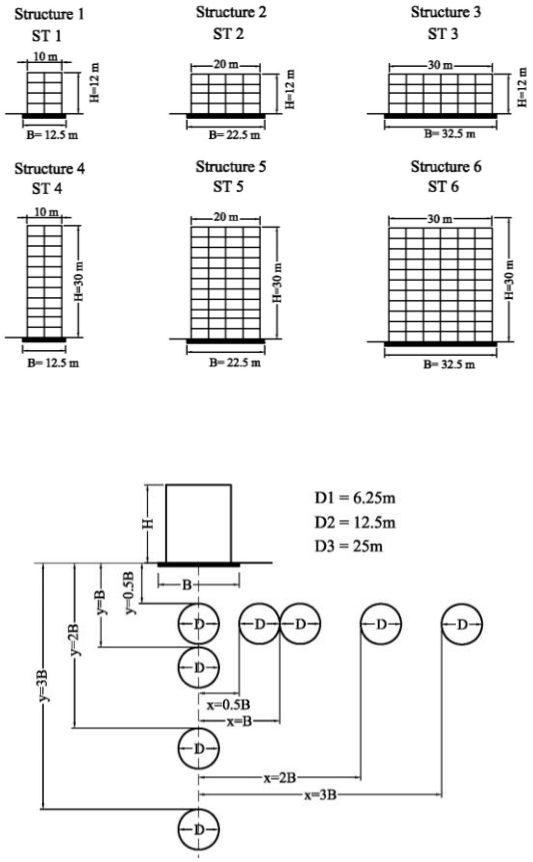


**Figure 4:The problem geometry of structures studied, and all twenty-four void location cases studied for each structure.**

#### 2.4.2 Parameters and Materials

The behavior of the structure constructed on soils containing voids is affected by the void location and its diameter. Three diameters of void were used (*D*= 6.25, 12.5, and 25 m) in this parametric study. Figure 4 shows the twenty-four most critical void locations that were selected to identify the critical void location under structures subjected to seismic loads for each structure. The material properties for clay foundation soil as follows: Modulus of elasticity *E*= 40 Mpa, Poisson ratio $v$ = 0.4, Soil cohesion $c$ = 40 kpa, Internal friction and Dilation angles are set to be zero $\varphi = \psi = 0$, and dry unit weight of the soil=17.2 kN/$m^3$.

Concrete properties as follows: Modulus of elasticity *E*= 30,000 Mpa, Poisson ratio $v$ = 0.2, and dry unit weight of the soil=22.5 kN/$m^3$.

Steel properties as follows: Modulus of elasticity *E*= 200,000 Mpa, Poisson ratio $v$ = 0.3, and dry unit weight of the soil=76.5 kN/$m^3$.

All examined RC structures were subjected to a lateral static load equivalent to the calculated seismic load as mentioned in the following section.

### 2.4.3 Lateral Loads Calculations

The six structures investigated by FEM were subjected to seismic loads by applying static lateral loads at the floor level. The equivalent static base shear was adopted as per the ECP-201 [42] with triangle vertical distribution pattern. The computed lateral load was distributed at floor levels at the mass center according to the floor height $H_i$. Table 2 shows the distribution of lateral forces on each floor according to ECP-201 [42] for all the structures.

**Table 2.Distributed lateral loads at floor levels for all the structures (in kPa)**

| $F_i$ | $H_i$ | ST 1 | ST 2 | ST 3 |
|---|---|---|---|---|
| $F_1$ | 3 | 31.1 | 124.4 | 279.8 |
| $F_2$ | 6 | 62.2 | 248.7 | 559.6 |
| $F_3$ | 9 | 93.3 | 373.1 | 839.4 |
| $F_4$ | 12 | 124.4 | 497.4 | 1119.2 |
| $\sum F_i$ | | **311** | **1243.6** | **2798** |

| $F_i$ | $H_i$ | ST 4 | ST 5 | ST 6 |
|---|---|---|---|---|
| $F_1$ | 3 | 13.2 | 52.8 | 118.9 |
| $F_2$ | 6 | 26.4 | 105.7 | 237.8 |
| $F_3$ | 9 | 39.6 | 158.5 | 356.7 |
| $F_4$ | 12 | 52.8 | 211.4 | 475.6 |
| $F_5$ | 15 | 66.1 | 264.2 | 594.4 |
| $F_6$ | 18 | 79.3 | 317.0 | 713.3 |
| $F_7$ | 21 | 92.5 | 369.9 | 832.2 |
| $F_8$ | 24 | 105.7 | 422.7 | 951.1 |
| $F_9$ | 27 | 118.9 | 475.6 | 1070 |
| $F_{10}$ | 30 | 132.1 | 528.4 | 1188.9 |
| $\sum F_i$ | | **726.6** | **2906.2** | **6538.9** |

## 3 RESULTS AND DISCUSSION

### 3.1 Linear Modal Analysis

A linear modal analysis for the first ten mode frequencies were performed. Two structures were used in this analysis ST1 with 12m and ST4 with 30 m heights. Also, the effect on building vibration frequencies in higher modes is greater than it in the fundamental mode of vibration. The analysis showed that the greatest effect on building natural frequency when the void center lines lie on building axis of symmetry, Figure 5. The effect of void almost be negligible when the void distance from building axis is greater than 1.5 building width either in vertical or in horizontal directions. The results also showed that when the void diameter is less than quarter building width the effect of void on building vibrations could be neglected. The maximum variation of building vibrations due to the presence of void is about 10% or less. Referring to Figure 6, the effect of void on building frequencies in buildings with small heights is much more than it in taller buildings.

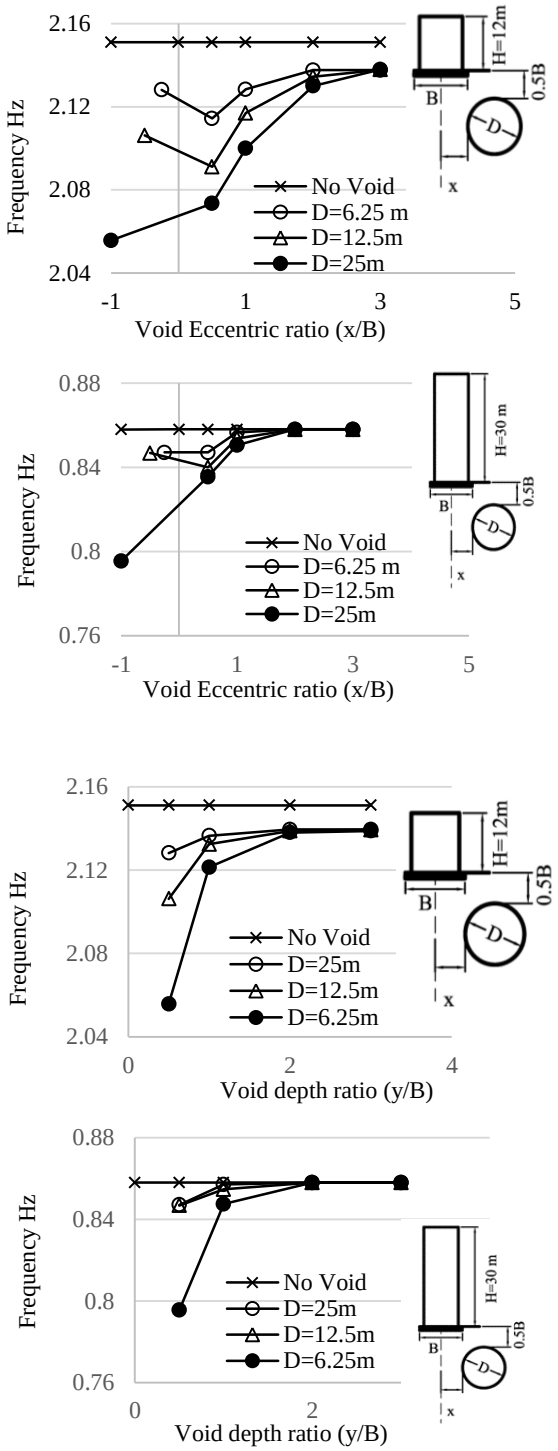


**Figure 5: Effect of void position on fundamental natural frequency of buildings**

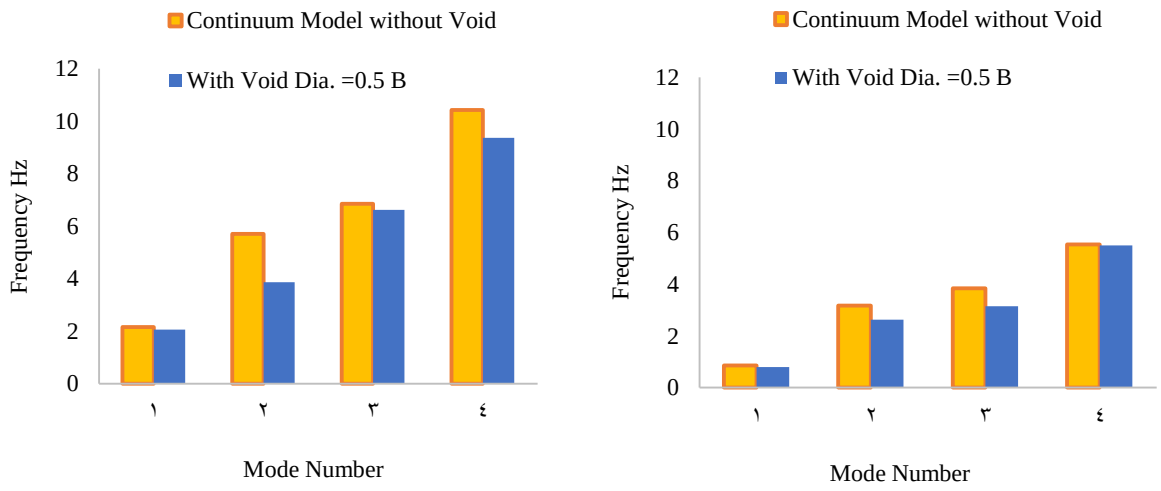


**(a) *H*= 12 m** **(b) *H*=30 m**

**Figure 6: Comparison between first 4 frequencies for different cases of support modeling**

### 3.2 Lateral Displacement

Based on the results, it was found that the presence of underground voids under the structures subjected to seismic loads cause an obvious increase in lateral displacements at the foundation and the floor levels compared to the case of no voids. This increase depends on the void's diameter and its location from the structure. Figures 7-9 show the lateral displacements at floor levels of the six investigated structures for all three void diameters in all effective location cases as shown in the figures. It was noticed that the lateral displacements at the foundation level and floor levels increase with the increase in the void diameter and the decrease in the void eccentric ratio ($x/B$) from the footing center.

From the results, the critical void location under the structures that causes an increase in lateral displacement values was computed for each structure. The void effect was neglected at about 3 % change compared to the no-void case. For structure ST 1, the critical eccentric ratios ($x_{cr}/B$) are 1.25, 1.75, and 2 for the void diameter $D$ of 6.25m, 12.5m, and 25m, respectively. For structures ST 2, ST 3, ST 4 and ST 5, the critical eccentric ratios ($x_{cr}/B$) are 1, 1.5, and 1.75 for the void diameter $D$ of 6.25m, 12.5m, and 25m, respectively. For structure ST 6, the critical eccentric ratios ($x_{cr}/B$) are 0.5, 0.75, and 1.5 for the void diameter $D$ of 6.25m, 12.5m, and 25m, respectively. These results can be classified into three categories, upper bound condition for structure ST 1, medium bound condition for structures ST 2, ST 3, ST 4, and ST 5, and lower bound condition for structure ST 6 as shown in Figure 11a. This is because structure ST 1 of less height and width is more amenable to lateral displacement due to underground voids than other structures that have stability by their weight. On the other side, structure ST 6, the highest and the broadest structure is the most stable against lateral loads.

### 3.3 The Inter-Story Drift

Figures 7-9 show the Inter-story drift values for the six structures with different void diameters and their locations. It was found that inter-story drift values increase also as the void diameter $D$ increases and the void eccentric ratio ($x/B$) from the footing center decreases.

In the case of a void located exactly centric under the footing, the increase of lateral displacements of the structure was almost the same as the no-void condition, although the inter-story drift values slightly increased with the increase in the void diameter. The increase in these values was evident in the case of high structures for the same case.

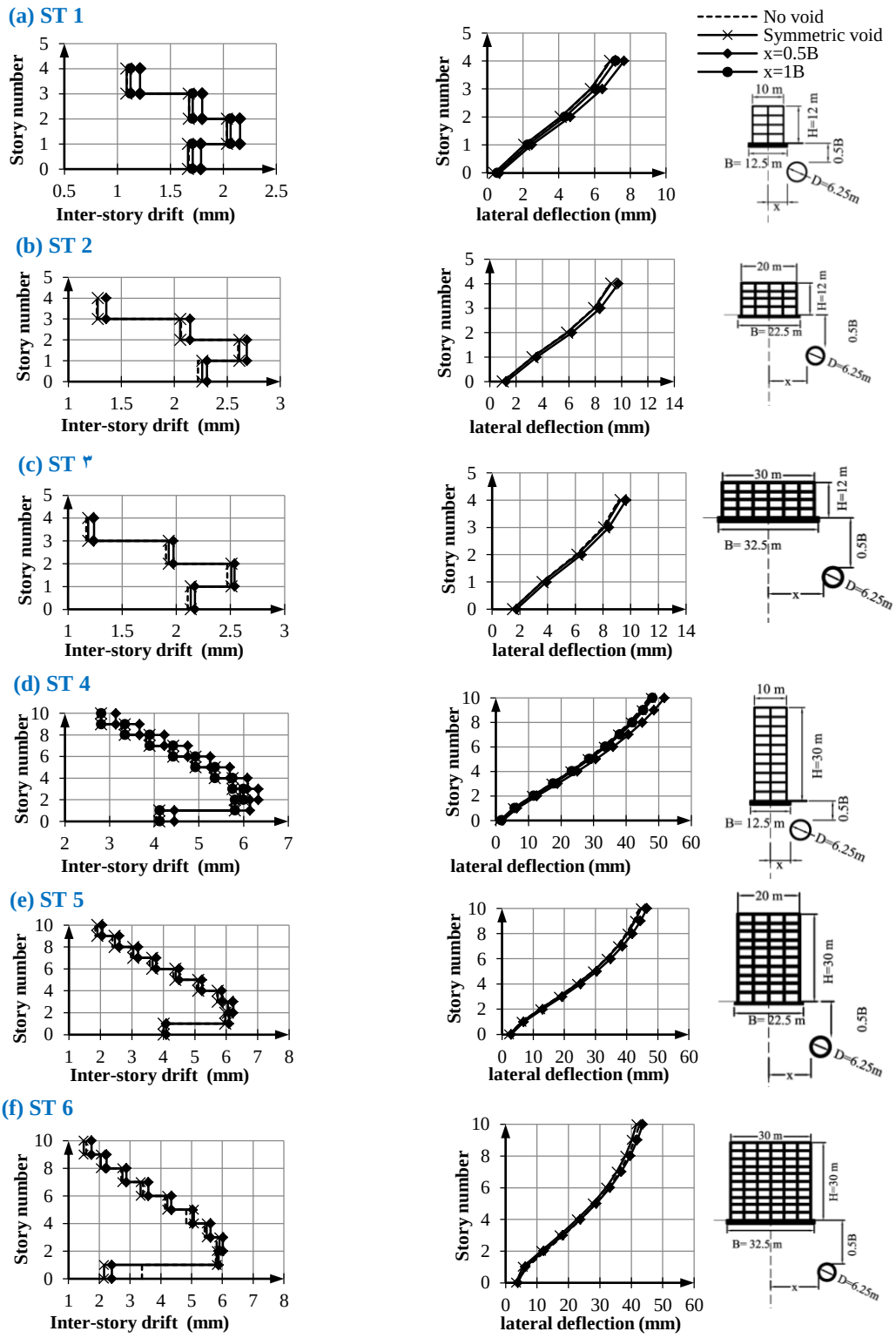


**Figure 7: Lateral deflection and Inter-story drift for *D*=6.25m; (a) ST 1, (b) ST 2, (c) ST 3, (d) ST 4, (e) ST 5, and (f) ST 6.**

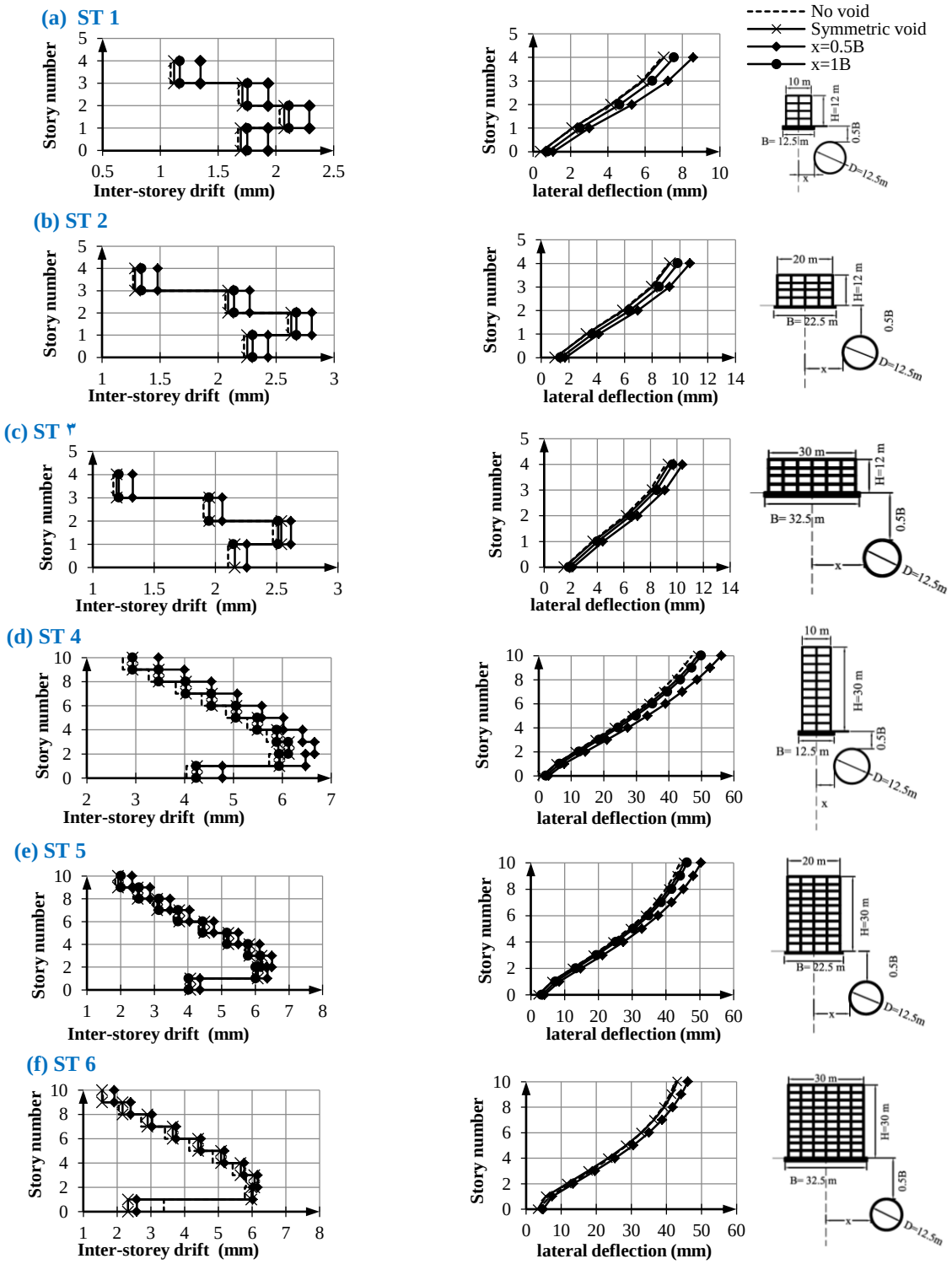


**Figure 8: Lateral deflection and Inter-story drift for *D*=12.5m; (a) ST 1, (b) ST 2, (c) ST 3, (d) ST 4, (e) ST 5, and (f) ST 6.**

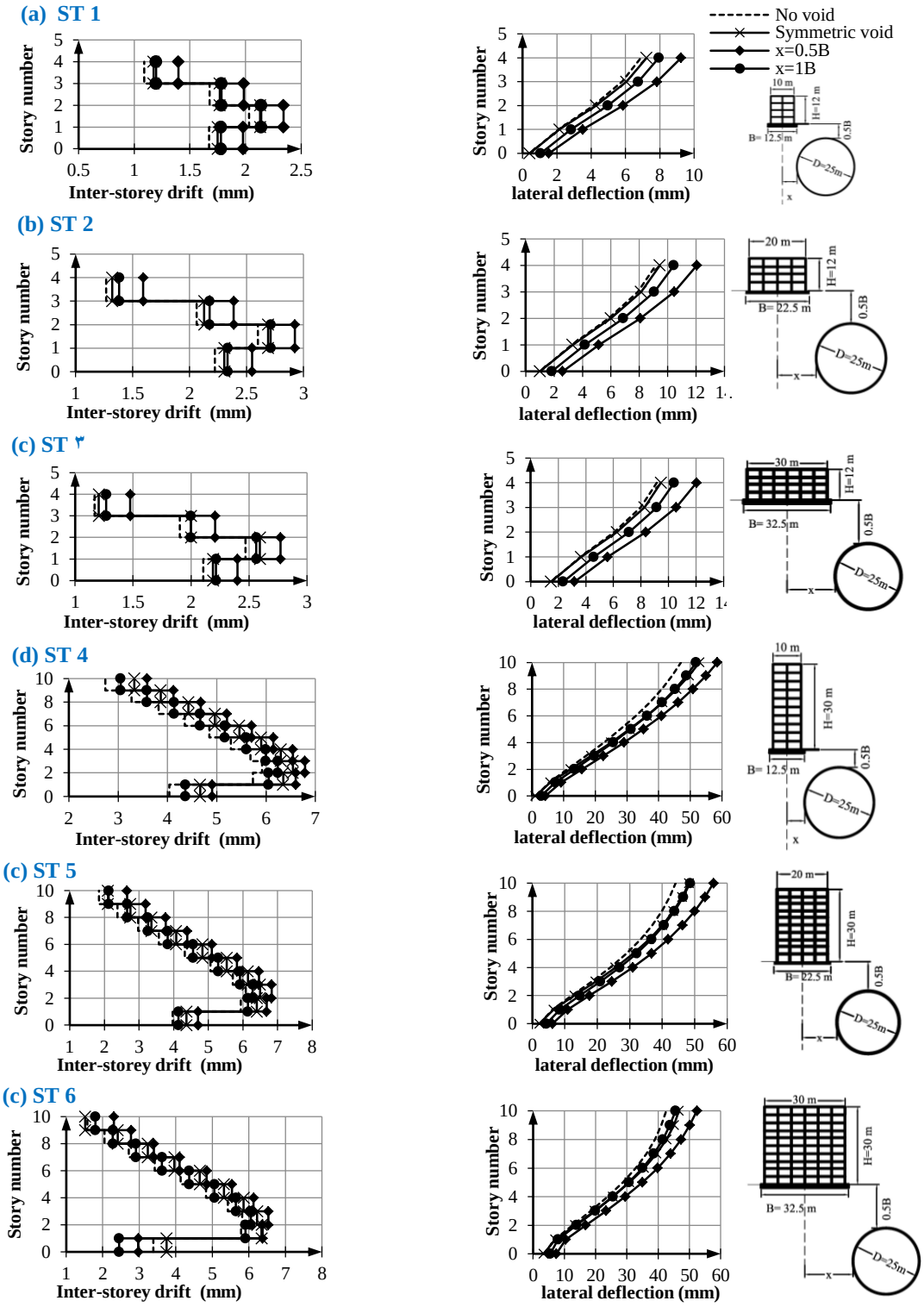


**Figure 9: Lateral deflection and Inter-story drift for *D*=25m; (a) ST 1, (b) ST 2, (c) ST 3, (d) ST 4, (e) ST 5, and (f) ST 6.**

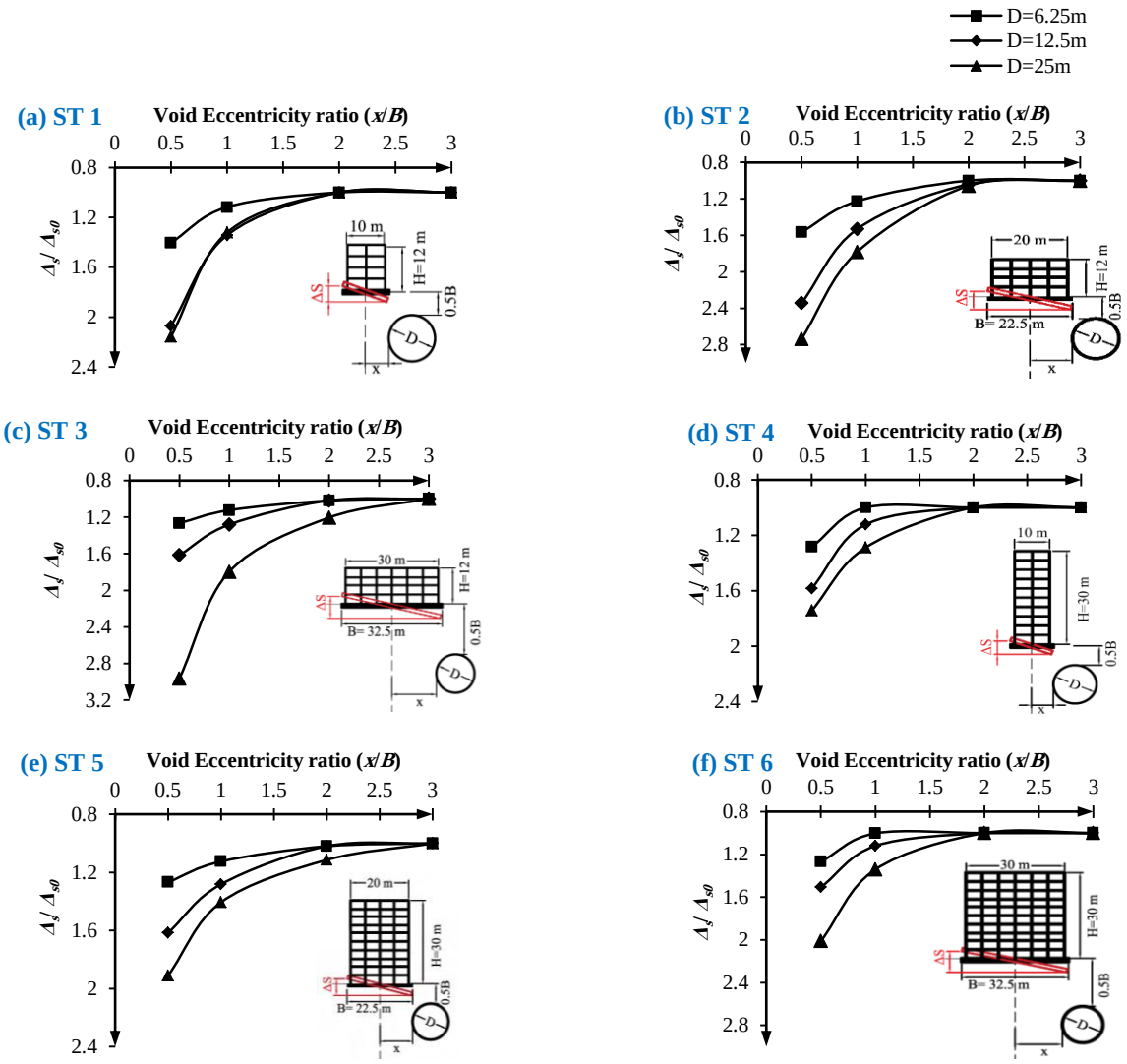


**Figure 10: Differential displacement ratios $\Delta s/\Delta s_0$; (a) ST 1, (b) ST 2, (c) ST 3, (d) ST 4, (e) ST 5, and (f) ST 6.**

### 3.4 Differential Settlement under Footings

The differential settlement under the footings was affected by underground voids depending on the void size and its location. It was found that the differential settlement under the footings increases as the void diameter increases and as the void distance from the footings decreases, as shown in Figure 10. It was also noticed that for the same structure width B, as the structure height $H$ increases the effect of voids in differential settlement under the footings decreases. The void effect was neglected at about 3 % change compared to the no-void case in terms of differential settlement ratio $\Delta s/\Delta s_0$ to get the critical eccentric ratios ($x_{cr}/B$) for each structure. Where;

$\Delta s$: The differential settlement of the footing resting on void,

$\Delta s_0$: The differential settlement of the footing in case of no-void.

First, the three structures having the same height $H$ of 12m were compared, as shown in Figure 11b. For structure ST 1, the critical eccentric ratios ($x_{cr}/B$) are 1.75, 2, and 2 for the void diameter $D$ of 6.25m, 12.5m, and 25m, respectively. For structure ST 2, the critical eccentric ratios ($x_{cr}/B$) are 2, 2, and 2.5 for the void diameter $D$ of 6.25m, 12.5m, and 25m, respectively. For structure ST 3, the critical eccentric ratios ($x_{cr}/B$) are 1, 2, and 3 for the void diameter $D$ of 6.25m, 12.5m, and 25m, respectively. It was found that as the structure width increases, the differential settlement ratios $\Delta s/\Delta s_0$ increase. It was found that structure ST 3 with void diameter $D$ =6.25m showed a critical eccentric ratio ($x_{cr}/B$) less than structures ST 1 and ST 2. That means, in low-rise structures, the critical eccentric ratios ($x_{cr}/B$) increase with increasing the structure width $B$, except in the small voids compared to the structure's width $D/B$, the void effect in the differential settlement term decreases. Second, the three structures having the same

height $H$ of 30m were compared, as shown in Figure 11c. For structure ST 4, the critical eccentric ratios ($x_{cr}/B$) are 1, 2, and 2 for the void diameter $D$ of 6.25m, 12.5m, and 25m, respectively. For structure ST 5, the critical eccentric ratios ($x_{cr}/B$) are 1.5, 2, and 2.5 for the void diameter $D$ of 6.25m, 12.5m, and 25m, respectively. For structure ST 6, the critical eccentric ratios ($x_{cr}/B$) are 1, 1.75, and 2 for the void diameter D of 6.25m, 12.5m, and 25m, respectively. In high-rise structures having the same height $H$ of 30m, the differential settlement ratios $\Delta s/\Delta s_0$ increase as the structure's width $B$ increases. Although it was found that structure ST 6 shows less void effect because of its high stability compared to other investigated structures.

### 3.5 Maximum Settlement

Settlements under the footings of the structures were obtained from the ANSYS analysis. The maximum settlement values under each structure's raft were compared with the no-void case. Centric voids under footings don't cause an increase in the footing differential settlement or lateral displacements at the floor levels. For this reason, the change of the maximum settlement values under the foundations was only considered to get the critical void depth ratio ($y_{cr}/B$). From the results, the critical void depth ratio for the structures subjected to lateral seismic loads was considered at about 3 % change compared to the no-void case. For structures ST 1 and ST 4, the critical void depth ratios ($y_{cr}/B$) are 2, 3, and 3.5 for the void diameter $D$ of 6.25m, 12.5m, and 25m, respectively. For structures ST 2 and ST 5, the critical void depth ratios ($y_{cr}/B$) are 1.5, 2, and 3 for the void diameter $D$ of 6.25m, 12.5m, and 25m, respectively. For structures ST 3 and ST 6, the critical void depth ratios ($y_{cr}/B$) are 1, 1.5, and 2 for the void diameter $D$ of 6.25m, 12.5m, and 25m, respectively, as shown in Figure 11d.

### 3.6 Critical Void Locations

Critical void locations below the investigated structures ($y_{cr}/B$ and $x_{cr}/B$) in which voids can affect the surface structures above were classified into three zones according to the loading type and the void effects. Figure 12 shows the critical void zones, red, green, and blue zones. The red zone represents the critical void zone when the structure is subjected to gravity loads only. If the structure is subjected to seismic loads, the critical zone increases up to the end of the blue zone. The green critical zone represents the effects of the underground voids concerning the lateral displacements of the structures. The blue critical zone represents the effects of the underground voids concerning the footing differential settlement. It was shown that critical void depth ($y_{cr}/B$) is the same in both loading cases. Critical void eccentricity ($x_{cr}/B$) increases as the structure's width B increases. On the other hand, it was noticed that as the structure's height H increases, the critical void eccentricity ($x_{cr}/B$) decreases, because the structure's stability against the lateral loading increases and the effects of the voids on the above structures decrease.

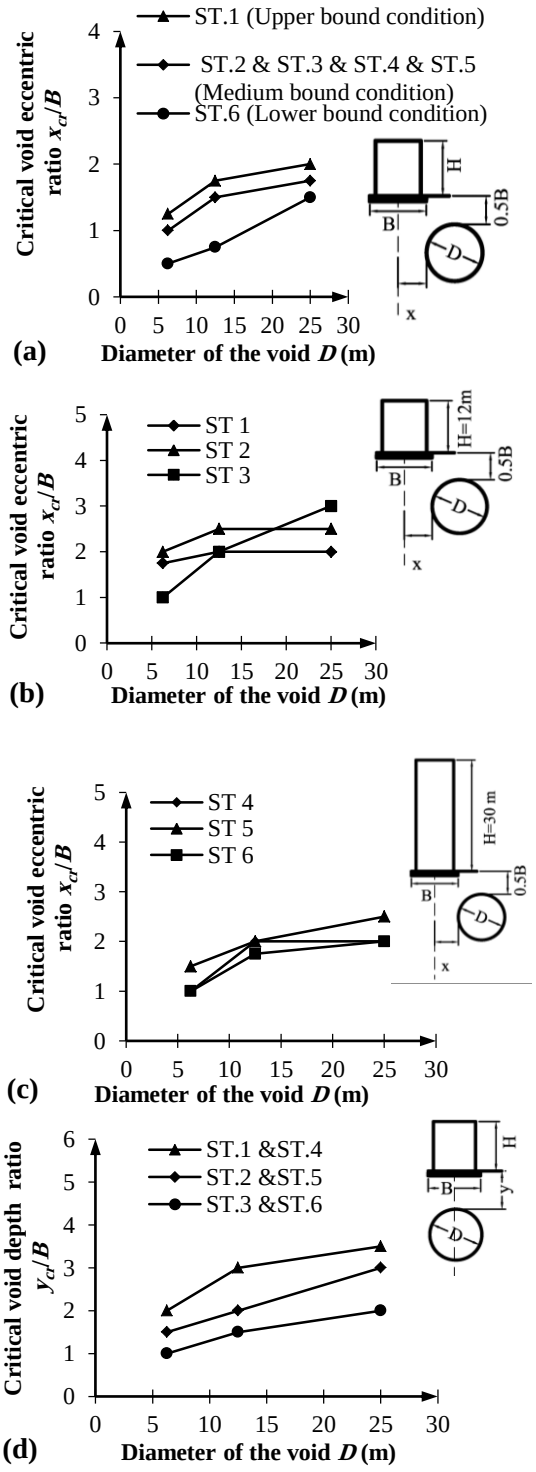


**Figure 11: Critical eccentric void location; (a) $x_{cr}/B$ for a comparison of lateral displacement at structure's top, (b) $x_{cr}/B$ for a comparison of differential settlement for ST1&ST2&ST3 of 12m height, (c) $x_{cr}/B$ for a comparison of differential settlement for ST4&ST5&ST6 of 30m height, and (d) Critical void depth ratios ($y_{cr}/B$).**

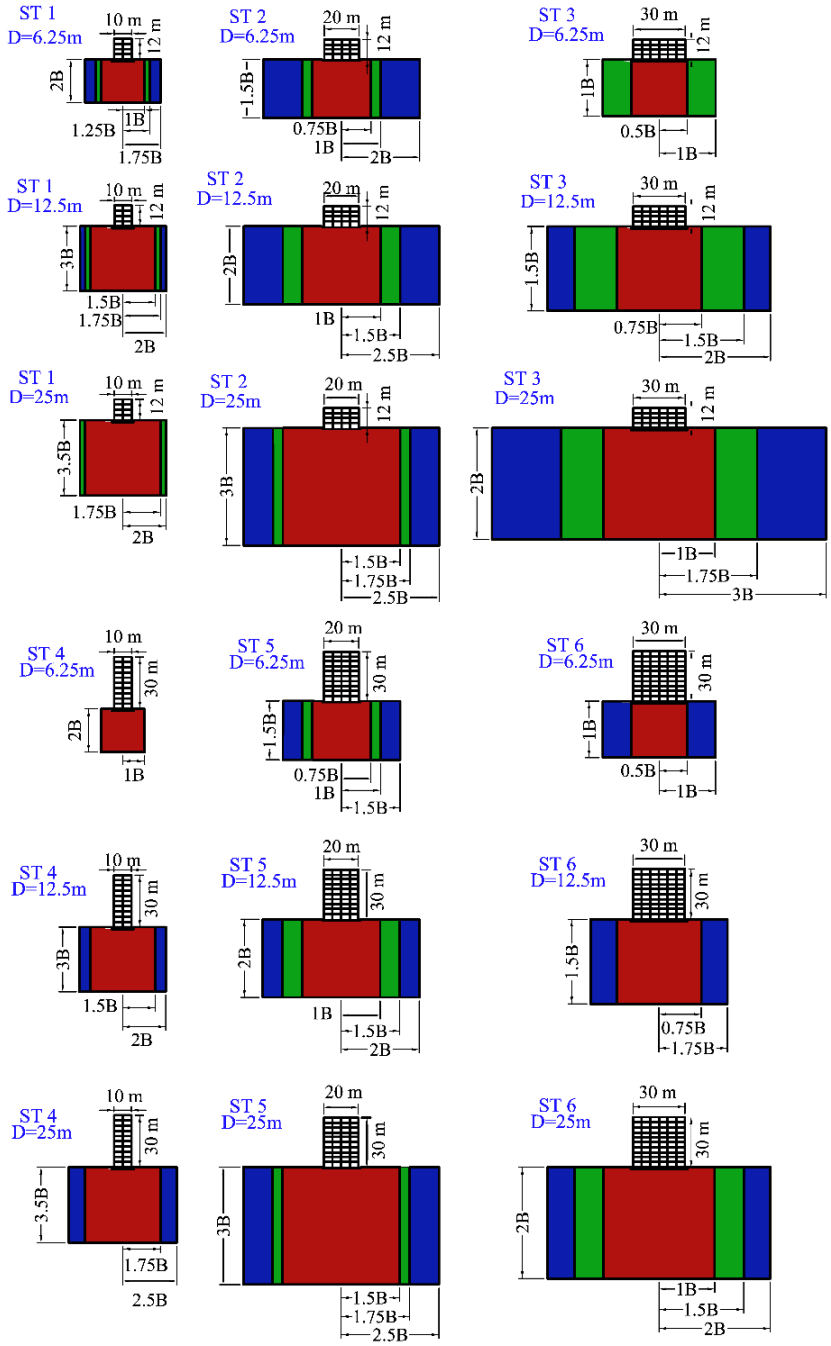


**Figure 12: Critical void locations for the structures, red zone: under static loads, green zone: under equivalent seismic loads according to the change in lateral displacement at the structure's top, and blue zone: under equivalent seismic loads according to the change in footing differential settlement**

## 4 CONCLUSIONS

Three-dimensional finite element modeling was performed using the ANSYS software. This analysis investigated the behavior of the RC surface structures founded on clay soils containing an underground void in an unknown location under seismic loads. Two cases study were chosen to validate the ANSYS model under static and dynamic loading. Six reinforced concrete buildings were analyzed with different areas and heights. Each building was analyzed under twenty-four cases of void location and diameter.

According to the cases studied, it was concluded that:

- Presence of underground voids under RC structures causes an increase in lateral displacements at the foundation level and floor levels compared to the no-void case. This change in lateral displacement increases as the void's diameter *D* increases and the

void eccentricity ($x/B$) from the footing center decreases.

- The inter-story drift values increase as the void's diameter $D$ increases and the void eccentric ratio ($x/B$) from the footing center decreases.
- The differential settlement under the footings increases with increasing the void diameter $D$ and decreasing the void eccentric ratio ($x/B$) from the footing center. The effect of the presence of voids in increasing the differential settlement under the footing is more apparent in structures with wider widths.
- For the structures with the same structure width, as the structure's height $H$ increases, the effect of voids in differential settlement under the footings decreases.
- Centric voids under footings don't cause an increase of footing differential settlement or lateral displacements at the floor level compared to the no-void case.
- Charts were presented for predicting the behavior of the structures above the soil with voids for a wide range of parameters under seismic loads. The charts include the void effects on the maximum settlement under the footing, footing differential settlement, inter-story drift, and lateral displacement at the floor levels.
- Charts for estimating the critical void locations under the foundations were presented depending on structure size, void size, and void location. Change in differential settlement under footings due to underground voids is the most influential in the critical void region estimation under the foundations subjected to seismic loads.

There is still a need for investigating many other parameters in this field, such as using different types of soil, different void shapes, and foundation types under seismic loads. Applying ground accelerations in the ANSYS model is also recommended to investigate their effects on the critical void locations estimation.

## REFERENCES


[1] J. K. Lee, S. Jeong, and J. Ko, "Undrained stability of surface strip footings above voids," *Computers and Geotechnics*, vol. 62, pp. 128-135, 2014. https://doi.org/10.1016/j.compgeo.2014.07.009

[2] R. L. Baus, *The stability of shallow continuous footings located above voids*: The Pennsylvania State University, 1980. https://doi.org/10.1061/(ASCE)0733-9410(1983)109:1(1).

[3] R. Baus, and M. Wang, "Bearing capacity of strip footing above void," *Journal of Geotechnical Engineering*, vol. 109, no. 1, pp. 1-14, 1983. https://doi.org/10.1061/(ASCE)0733-9410(1983)109:1(1).

[4] M. Wang, and A. Badie, "Effect of underground void on foundation stability," *Journal of Geotechnical Engineering*, vol. 111, no. 8, pp. 1008-1019, 1985. https://doi.org/10.1061/(asce)0733-9410(1985)111:8(1008).

[5] M. Wang, and C. Hsieh, "Collapse load of strip footing above circular void," *Journal of geotechnical engineering*, vol. 113, no. 5, pp. 511-515, 1987.

[6] M. Wang, C. Yoo, and C. Hsieh, "Effect of void on footing behavior under eccentric and inclined loads." pp. 1226-1239.

[7] A. Badie, and M. Wang, "Stability of Underground Cavity subjected to Surface Loads."

[8] C. Hsieh, "Footing behavior and stability analysis method for strip surface footing above continuous circular void," 1992.

[9] C. Hsieh, and M. Wang, "Bearing capacity determination method for strip surface footings underlain by voids," *Transportation Research Record*, no. 1336, 1992.

[10] V. Lee, S. Chen, and I. Hsu, "Antiplane diffraction from canyon above subsurface unlined tunnel," *Journal of Engineering Mechanics*, vol. 125, no. 6, pp. 668-675, 1999. https://doi.org/10.1061/(ASCE)0733-9399(1999)125:6(668)

[11] M. Kiyosumi, O. Kusakabe, M. Ohuchi *et al.*, "Yielding pressure of spread footing above multiple voids," *Journal of Geotechnical and Geoenvironmental Engineering*, vol. 133, no. 12, pp. 1522-1531, 2007. https://doi.org/10.1061/(asce)1090-0241(2007)133:12(1522).

[12] M. Kiyosumi, O. Kusakabe, and M. Ohuchi, "Model tests and analyses of bearing capacity of strip footing on stiff ground with voids," *Journal of geotechnical and geoenvironmental engineering*, vol. 137, no. 4, pp. 363-375, 2011. https://doi.org/10.1061/(ASCE)GT.1943-5606.0000440.

[13] M. M. A. Hussein, "Stability of strip footing on sand bed with circular void," *JES. Journal of Engineering Sciences*, vol. 42, no. 1, pp. 1-17, 2014.https://doi.org/10.21608/jesaun.2014.111011.https://doi.org/10.21608/jesaun.2014.111011.

[14] A. A. Lavasan, A. Talsaz, M. Ghazavi *et al.*, "Behavior of shallow strip footing on twin voids," *Geotechnical and Geological Engineering*, vol. 34, pp. 1791-1805, 2016. https://doi.org/10.1007/s10706-016-9989-6.

[15] H. Zhou, G. Zheng, X. He *et al.*, "Bearing capacity of strip footings on c–φ soils with

square voids," *Acta Geotechnica*, vol. 13, pp. 747-755, 2018. https://doi.org/10.1007/s11440-018-0630-0.

[16] L. Zhao, S. Huang, R. Zhang *et al.*, "Stability analysis of irregular cavities using upper bound finite element limit analysis method," *Computers and Geotechnics*, vol. 103, pp. 1-12, 2018. .https://doi.org/10.1016/j.compgeo.2018.06.018

[17] J. K. Lee, and J. Kim, "Stability charts for sustainable infrastructure: Collapse loads of footings on sandy soil with voids," *Sustainability*, vol. 11, no. 14, pp. 3966, 2019. https://doi.org/10.3390/su11143966.

[18] G. Wu, M. Zhao, H. Zhao *et al.*, "Effect of eccentric load on the undrained bearing capacity of strip footings above voids," *International Journal of Geomechanics*, vol. 20, no. 7, pp. 04020078, 2020. https://doi.org/10.1061/(ASCE)GM.1943-5622.0001710.

[19] S. Anaswara, and R. Shivashankar, "Study on behaviour of two adjacent strip footings on granular bed overlying clay with a void," *Transportation Infrastructure Geotechnology*, vol. 7, pp. 461-477, 2020. https://doi.org/10.1007/s40515-020-00122-x.

[20] M. S. Islam, and M. Iskander, "Twin tunnelling induced ground settlements: A review," *Tunnelling and Underground Space Technology*, vol. 110, pp. 103614, 2021. https://doi.org/10.1016/j.tust.2020.103614

[21] M. S. Islam, and M. Iskander, "Effect of Geometric Parameters and Construction Sequence on Ground Settlement of Offset Arrangement Twin Tunnels," *Geosciences*, vol. 12, no. 1 pp. 41, 2022. https://doi.org/10.3390/geosciences12010041

[22] M. S. Islam, and M. Iskander, "Ground settlement caused by perpendicularly crossing twin tunnels, a parametric study," *Tunnelling and Underground Space Technology*, vol. 146, pp.105657, 2024. https://doi.org/10.1016/j.tust.2024.105657

[23] T. Mansouri, R. Boufarh, and D. Saadi, "Effects of underground circular void on strip footing laid on the edge of a cohesionless slope under eccentric loads," *Soils and Rocks*, vol. 44, 2021. https://doi.org/10.28927/SR.2021.055920

[24] B. Mazouz, T. Mansouri, M. Baazouzi *et al.*, "Assessing the Effect of Underground Void on Strip Footing Sitting on a Reinforced Sand Slope with Numerical Modeling," *Engineering, Technology & Applied Science Research*, vol. 12, no. 4, pp. 9005-9011, 2022. .https://doi.org/10.48084/etasr.5131

[25] B. Das, and K. Khing, "Foundation on layered soil with geogrid reinforcement—effect of a void," *Geotextiles and Geomembranes*, vol. 13, no. 8, pp. 545-553, 1994. https://doi.org/10.1016/0266-1144(94)90018-3.

[26] S. Sireesh, T. Sitharam, and S. K. Dash, "Bearing capacity of circular footing on geocell–sand mattress overlying clay bed with void," *Geotextiles and Geomembranes*, vol. 27, no. 2, pp. 89-98, 2009. https://doi.org/10.1016/j.geotexmem.2008.09.005

[27] S. Moghaddas Tafreshi, O. Khalaj, and M. Halvaee, "Experimental study of a shallow strip footing on geogrid-reinforced sand bed above a void," *Geosynthetics International*, vol. 18, no. 4, pp. 178-195, 2011. https://doi.org/10.1680/gein.2011.18.4.178.

[28] J. P. Sahoo, and J. Kumar, "Seismic stability of a long unsupported circular tunnel," *Computers and Geotechnics*, vol. 44, pp. 109-115, 2012. https://doi.org/10.1016/j.compgeo.2012.03.015

[29] A. Asakereh, M. Ghazavi, and S. M. Tafreshi, "Cyclic response of footing on geogrid-reinforced sand with void," *Soils and foundations*, vol. 53, no. 3, pp. 363-374, 2013. https://doi.org/10.1016/j.sandf.2013.02.008

[30] D. Chakraborty, and J. Kumar, "Stability of a long unsupported circular tunnel in soils with seismic forces," *Natural Hazards*, vol. 68, pp. 419-431, 2013. https://doi.org/10.1007/s11069-013-0633-y

[31] D. Chakraborty, and A. S. Sawant, "Seismic bearing capacity of strip footing above an unsupported circular tunnel in undrained clay," *International Journal of Geotechnical Engineering*, vol. 11, no. 1, pp. 97-105, 2017. https://doi.org/10.1080/19386362.2016.1185586

[32] R. Zhang, M. Feng, Y. Xiao *et al.*, "Seismic Bearing Capacity for Strip Footings on Undrained Clay with Voids," *Journal of Earthquake Engineering*, vol. 26, no. 9, pp. 4910-4923, 2022. https://doi.org/10.1080/13632469.2020.1851316

[33] M. Sadegh Es-haghi, M. Abbaspour, H. Abbasianjahromi *et al.*, "Machine learning-based prediction of the seismic bearing capacity of a shallow strip footing over a void in heterogeneous soils," *Algorithms*, vol. 14, no. 10, pp. 288, 2021. https://doi.org/10.3390/a14100288

[34] M. Jao, and M. Wang, "Stability of strip footings above concrete-lined soft ground tunnels," *Tunnelling and Underground Space Technology*, vol. 13, no. 4, pp. 427-434, 1998. https://doi.org/10.1016/S0886-7798(98)00085-6

[35] H. Mroueh, and I. Shahrour, "A full 3-D finite element analysis of tunneling–adjacent

structures interaction," *Computers and Geotechnics*, vol. 30, no. 3, pp. 245-253, 2003. https://doi.org/10.1016/S0266-352X(02)00047-2

[36] A. Mirhabibi, and A. Soroush, "Effects of surface buildings on twin tunnelling-induced ground settlements," *Tunnelling and Underground Space Technology*, vol. 29, pp. 40-51, 2012. https://doi.org/10.1016/j.tust.2011.12.009

[37] D. Boldini, N. Losacco, S. Bertolin *et al.*, "Finite element modelling of tunnelling-induced displacements on framed structures," *Tunnelling and underground space technology*, vol. 80, pp. 222-231, 2018. https://doi.org/10.1016/j.tust.2018.06.019

[38] A. G. Abdel-Nasser, E. Abdel-Galil, and E. A. Sallam, "Numerical Assessment of RC Building Deformations Resting on Soil Containing Voids with Various Sizes and Locations," *Port-Said Engineering Research Journal*, vol. 27, no. 4, pp. 1-15, 2023. https://doi.org/10.21608/pserj.2023.226664.1254

[39] K. Pitilakis, G. Tsinidis, A. Leanza *et al.*, "Seismic behaviour of circular tunnels accounting for above ground structures interaction effects," *Soil Dynamics and Earthquake Engineering*, vol. 67, pp. 1-15, 2014. https://doi.org/10.1016/j.soildyn.2014.08.009

[40] G. Abate, and M. R. Massimino, "Parametric analysis of the seismic response of coupled tunnel–soil–aboveground building systems by numerical modelling," *Bulletin of Earthquake Engineering*, vol. 15, pp. 443-467, 2017. https://doi.org/10.1007/s10518-016-9975-7

[41] G. Wang, M. Yuan, Y. Miao *et al.*, "Experimental study on seismic response of underground tunnel-soil-surface structure interaction system," *Tunnelling and Underground Space Technology*, vol. 76, pp. 145-159, 2018. https://doi.org/10.1016/j.tust.2018.03.015

[42] ECP201, *The Egyptian code for calculating loads and forces in construction and building works*, National Housing and Building Research Center: Cairo, Egypt, 2008.

[43] X. Gu, X. Jin, and Y. Zhou, *Basic principles of concrete structures*: Springer, 2016.

[44] A. Badie, " Stability of spread footing supported by clay soil with an underground void," 1984.